NSF-KITP 09-42

Angle resolved photon spectrum and quasiparticle excitation spectrum in an exciton superfluid

Jinwu Ye[1], T. Shi[2] and Longhua Jiang [1]
[1] *Department of Physics, The Pennsylvania State University, University Park, PA, 16802, USA*
[2] *Institute of Theoretical Physics, Chinese Academy of Sciences, Beijing, 100080, China*
(Dated: April 16, 2009)

There have been extensive experimental search for possible exciton superfluid in semiconductor electron-hole bilayer systems below liquid Helium temperature. However, exciton superfluid are meta-stable and will eventually decay through emitting photons. Here we show that the light emitted from the excitonic superfluid has unique and unusual features not shared by any other atomic or condensed matter systems. We evaluate angle resolved photon spectrum, momentum distribution curve, energy distribution curve and quasiparticle excitation spectrum in the exciton superfluid and comment on relevant experimental data in both exciton and exciton-polariton systems.

1. Introduction. An exciton is a bound state of an electron and a hole. Exciton condensate was first proposed more than 3 decades ago as a possible ordered state in solids [1, 2, 3]. But so far, no exciton superfluid phase has been observed in any bulk semi-conductors. Recently, degenerate exciton systems have been produced by different experimental groups with different methods in quasi-two-dimensional semiconductor $GaAs/AlGaAs$ coupled quantum wells structure [4, 5, 6, 7, 8]. When the distance between the two quantum wells is sufficiently small, an electron in the conduction band in one quantum well and a hole in the valence band in the other quantum well could pair to form an indirect exciton which behaves as a boson in dilute exciton density limit. It was established that the indirect excitons in EHBL has at least the following advantages over the excitons in the bulk: (1) Due to the space separation of electrons and holes, the lifetime τ_{ex} of the indirect excitons is $10^3 \sim 10^5$ longer than that of direct ones, now it can be made as long as microseconds. (2) Due to the relaxation of the momentum conservation along the $\hat{z}$ direction, the thermal lattice relaxation time τ_L of the indirect excitons can be made as 10^{-3} that of bulk excitons, so $\tau_{ex} \gg \tau_L$ is well satisfied. (3) The repulsive dipole-dipole interaction is crucial to stabilize the excitonic superfluid against the competing phases such as bi-exciton formation and electron-hole plasma phase. So EHBL is a very promising system to observe BEC of in-direct excitons. The quantum degeneracy temperature of a two dimensional excitonic superfluid (ESF) can be estimated to be $T_d^{ex} \sim 3K$ for exciton density $n \sim 10^{10} cm^{-2}$ and effective exciton mass $m \sim 0.22 m_0$ where m_0 is the bare mass of an electron, so it can be reached easily by He refrigerator. Indeed, as temperature is decreased from $\sim 20K$ to $\sim 1.7K$, the spatially and spectrally resolved PL peak density centering around the gap $E_g \sim 1.545eV$ increases [4], the exciton cloud size decreases to $L \sim 30\mu m$, the peak width shrinking to $\sim 1meV$ at the lowest temperature $\sim 1.7K$. All these facts indicate a possible formation of exciton condensate around $1.7K$.

In this paper, we will study quantum nature of photons emitted from the excitonic superfluid phase in semiconductor electron-hole bilayer systems. We comment on current PL experimental data and also propose possible future experiments such as angle resolved power spectrum to test the existence of exciton condensate in the EHBL system. The phase sensitive homodyne measurement to detect the two mode squeezing spectrum and HanburyBrown-Twiss type of experiments to detect two photon correlations and photon statistics will be presented in a separate publication [11]. In this paper, for simplicity, we ignore the spins of excitons, the effects of a trap and disorders. Their effects are important and will be investigated in separate publications.

2. Exciton-Photon Hamiltonian. The total Hamiltonian in grand canonical ensemble is the sum of excitonic superfluid part, photon part and the coupling between the two parts $H_t = H - \mu N_t = H_{sf} + H_{ph} + H_{int}$ where :

$$\begin{aligned} H_{sf} &= \sum_{\vec{k}} (E^{ex}_{\vec{k}} - \mu) b^\dagger_{\vec{k}} b_{\vec{k}} + \frac{1}{2A} \sum_{\vec{k}\vec{p}\vec{q}} V_d(q) b^\dagger_{\vec{k}-\vec{q}} b^\dagger_{\vec{p}+\vec{q}} b_{\vec{p}} b_{\vec{k}} \\ H_{ph} &= \sum_k \omega_k a^\dagger_k a_k \\ H_{int} &= \sum_k [i g(k) a_k b^\dagger_{\vec{k}} + h.c.]. \end{aligned} \quad (1)$$

where A is the area of the EHBL, the exciton energy $E^{ex}_{\vec{k}} = \vec{k}^2/2M + E_g - E_b$, the photon frequency $\omega_k = v_g \sqrt{k_z^2 + \vec{k}^2}$ where $v_g = c/\sqrt{\epsilon}$ with c the light speed in the vacuum and $\epsilon \sim 12$ the dielectric constant of $GaAl$, $k = (\vec{k}, k_z)$ is the 3 dimensional momentum, $V_d(\vec{q}) = \frac{2\pi e^2}{\epsilon q}(1 - e^{-qd})$ is the dipole-dipole interaction between the excitons [12], $V_d(|\vec{r}| \gg d) = e^2 d^2 / |\vec{r}|^3$ and $V_d(q = 0) = \frac{2\pi e^2 d}{\epsilon}$ leads to a capacitive term for the density fluctuation [13]. The $g(k) \sim \vec{\epsilon}_{k\lambda} \cdot \vec{D}_k \times L_z^{-1/2}$ is the coupling between the exciton and the photons where

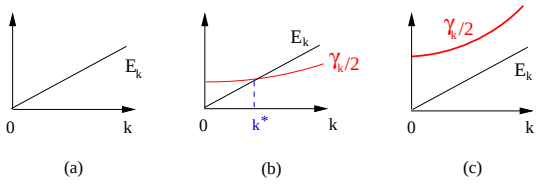

FIG. 1: The energy spectrum and the decay rate of the exciton versus in-plane momentum $\vec{k}$. (a) The energy spectrum of an equilibrium superfluid with $\tau_{ex} \to \infty$. (b) the indirect exciton superfluid with finite, but large τ_{ex} (c) The direct exciton with short τ_{ex}.

$L_z \to \infty$ is the normalization length along the z direction. Obviously, only the photon polarization in the plane spanned by k and $\vec{D}_{\vec{k}}$ contributes. Note that the transition dipole moment $\vec{D}_k$ from the conduction band to the valence band at a momentum k is completely different from the static dipole moment in the dipole-dipole interaction $V_d(\vec{q})$ in Eqn. 1.

In the dilute limit, V_d is relatively weak, so we can apply standard Bogoloubov approximation to this system. So in the ESF phase, one can decompose the exciton operator into the condensation part and the quantum fluctuation part above the condensation $b_{\vec{k}} = \sqrt{N}\delta_{\vec{k}0} + \tilde{b}_{\vec{k}}$. Upto the quadratic terms, the exciton Hamiltonian H_{sf} can be diagonalized by Bogoliubov transformation: $H_{sf} = E(0) + \sum_{\vec{k}} E(\vec{k})\beta^\dagger_{\vec{k}}\beta_{\vec{k}}$ where $E(0)$ is the condensation energy, $E(\vec{k}) = \sqrt{\epsilon_{\vec{k}}[\epsilon_{\vec{k}} + 2\bar{n}V_d(\vec{k})]}$, $\beta_{\vec{k}} = u_{\vec{k}}\tilde{b}_{\vec{k}} + v_{\vec{k}}\tilde{b}^\dagger_{-\vec{k}}$ is the Bogoliubov quasi-particle annihilation operators with the two coherence factors $u^2_{\vec{k}}(v^2_{\vec{k}}) = \frac{\epsilon_{\vec{k}} + \bar{n}V_d(\vec{k})}{2E(\vec{k})} \pm \frac{1}{2}$. The linear term in $\tilde{b}_k$ is eliminated by setting the chemical potential $\mu = E^{ex}_0 + \bar{n}V_d(0) = (E_g - E_b) + \bar{n}V_d(0)$. *In a stationary state, the μ is kept fixed at this value [14].* As $\vec{k} \to 0$, $E(\vec{k}) = u\left|\vec{k}\right|$ shown in Fig.1a where the velocity of the quasi-particle is $u = \sqrt{\bar{n}V_d(0)/M} = \sqrt{\frac{2\pi e^2 d\bar{n}}{\epsilon M}}$. Even at $T = 0$, the number of excitons out of the condensate is: $n'(T=0) = \frac{1}{S}\sum_{\vec{k}}\langle\tilde{b}^\dagger_{\vec{k}}\tilde{b}_{\vec{k}}\rangle = \int \frac{d^2\vec{k}}{(2\pi)^2}v^2_{\vec{k}}$ which is the quantum depletion of the condensate due to the dipole-dipole interaction.

We can decompose the interaction Hamiltonian H_{int} in Eqn.1 into the coupling to the condensate part $H^c_{int} = \sum_{k_z}[ig(k_z)(\sqrt{N} + \tilde{b}_0)a_{k_z} + h.c.]$ and to the quasi-particle part $H^q_{int} = \sum_k [ig(k)a_k\tilde{b}^\dagger_k + h.c.]$. In the following, we study $\vec{k} = 0$ and $\vec{k} \neq 0$ respectively.

3. The photon characteristics at the $\vec{k} = 0$ mode. The Heisenberg equation of motion of the photon annihilation operator is:

$$i\partial_t \langle a_{k_z}\rangle = (\omega_{k_z} - \mu - i\frac{\kappa}{2})\langle a_{k_z}\rangle - ig^*(k_z)\sqrt{N} \qquad (2)$$

where the average is over the initial zero photon state $|in\rangle = |BEC\rangle|0\rangle_{ph}$ and κ is the decay rate of the photon due to its coupling to a reservoir to be determined self-consistently. The stationary solution of Eqn.2 is [15]:

$$\langle a_{k_z}\rangle = \frac{ig^*(k_z)\sqrt{N}}{(\omega_{k_z} - \mu - i\kappa/2)}. \qquad (3)$$

which is the photon condensation induced by the exciton condensation at $\vec{k} = 0$ [16]. The photon number distribution is $n_{\omega_{k_z}} = \left\langle a^\dagger_{k_z}a_{k_z}\right\rangle = \frac{N|g(\mu/c)|^2}{(\omega_{k_z}-\mu)^2+\kappa^2/4}$ where we have set $g^*(k_z)$ around $\omega_{k_z} = \mu$. The total number of photons is $N_{ph} = \sum_{k_z} n_{\omega_{k_z}} = N(|g|^2D)/\kappa$ where $D = L_z/v_g$ is the photon density of states at $\vec{k} = 0$. Note that the exciton decay rate $\gamma_0 = |g|^2D$ at $\vec{k} = 0$ is independent of L_z, so is an experimentally measurable quantity. The N_{ph} has to be proportional to L_z in order to get a finite photon density in a given volume $L^2 \times L_z$ in a stationary state. This self-consistency condition sets $\kappa = v_g/L_z \to 0$ so that

$$n_{\omega_{k_z}} = N\gamma_0\delta(\omega_{k_z} - \mu), \quad N_{ph} = N\gamma_0 L_z/v_g \sim L_z \qquad (4)$$

which is independent of L_z as required. We showed that the power spectrum emitted from the exciton condensate has zero width. This conclusion is robust and is independent of any macroscopic details such as how photons are coupled to reservoirs. We conclude that the coherent light emitted from the condensate has the following remarkable properties: (1) highly directional: along the normal direction (1) highly monochromatic: pinned at a single energy given by the chemical potential μ (3) high power: proportional to the total number of excitons. These remarkable properties could be useful to build highly powerful opto-electronic device.

4. Input-Output formalism for a stationary state. Now we discuss the properties of emitted photons with non-zero in-plane momentum $\vec{k} \neq 0$. It is easy to see that due to the in-plane momentum conservation, the exciton with a fixed in-plane momentum $\vec{k}$ coupled to 3 dimensional photons with the same $\vec{k}$, but with different momenta k_z along the z-direction, so we can view these photon acting as the bath of the exciton by defining $\Gamma_{\vec{k}} = \sum_{k_z} g(k)a_k$. When using the standard input-output formalism which treats $g(k)$ non-perturbatively under Markov approximation [17], we find it is convenient to define the input and output fields as:

$$a^{in}_{\vec{k}}(t) = \sum_{k_z}\frac{1}{\sqrt{D_{\vec{k}}(\omega_k)}}a_k(t_0)e^{-i(\omega_k-\mu)(t-t_0)},$$
$$a^{out}_{\vec{k}}(t) = -\sum_{k_z}\frac{1}{\sqrt{D_{\vec{k}}(\omega_k)}}a_k(t_1)e^{-i(\omega_k-\mu)(t-t_1)}, \qquad (5)$$

where $t_0 \to -\infty$ and $t_1 \to \infty$ are the initial and final time respectively, so $t_0 < t < t_1$. The density of states of the photon with a given in-plane momentum $\vec{k}$ is $D_{\vec{k}}(\omega_k) = \frac{\omega_k L}{v_g\sqrt{\omega^2_k - v^2_g|\vec{k}|^2}}$. It can be shown that the

input and output fields obey the Bose commutation relations $[a^{in}_{\vec{k}}(t), a^{in\dagger}_{\vec{k}'}(t')] = [a^{out}_{\vec{k}}(t), a^{out\dagger}_{\vec{k}'}(t')] = \delta_{\vec{k},\vec{k}'}\delta(t-t')$.

By solving the Heisenberg equation of motion of Eqn.1, we find that the output field $a^{out}_{\vec{k}}(\omega)$ is related to the input field by:

$$a^{out}_{\vec{k}}(\omega) = [-1+\gamma_{\vec{k}}G_n(\vec{k},\omega+i\frac{\gamma_k}{2})]a^{in}_{\vec{k}}(\omega) + \gamma_{\vec{k}}G_a(\vec{k},\omega+i\frac{\gamma_k}{2})a^{in\dagger}_{-\vec{k}}(-\omega), \quad (6)$$

where the normal Green function $G_n(\vec{k},\omega) = i\frac{\omega+\epsilon_{\vec{k}}+\bar{n}V_d(\vec{k})}{\omega^2-E^2(\vec{k})}$ and the anomalous Green function $G_a(\vec{k},\omega) = \frac{i\bar{n}V_d(\vec{k})}{\omega^2-E^2(\vec{k})}$. The exciton decay rate in the two Green functions are $\gamma_{\vec{k}} = D_{\vec{k}}(\mu)\left|g_{\vec{k}}(\omega_k=\mu)\right|^2$ which is independent of L_z, so is an experimentally measurable quantity. Just from the rotational invariance, we can conclude that $\gamma_{\vec{k}} \sim const. + |\vec{k}|^2$ as $\vec{k}\to 0$ as shown in Fig.1b and 1c. Note that the Fourier transformation of the Eq. (5) leads to $\omega = \omega_k - \mu$. Eqn.6 can be considered as a S matrix relating the input photon field at $t_0 \to -\infty$ to the output photon field at $t_1 \to \infty$.

5. Photon number spectrum at $\vec{k}\neq 0$. The angle resolved power spectrum (ARPS) of the output field is $S_{\pm}(\vec{k},\omega) = \int_{-\infty}^{+\infty} d\tau e^{-i\omega\tau}\left\langle a^{out\dagger}_{\pm\vec{k}}(t+\tau)a^{out}_{\pm\vec{k}}(t)\right\rangle_{in}$. By inserting Eqn.6, one obtains $S_{\pm}(\vec{k},\omega) = S_1(\vec{k},\omega)$.

$$S_1(\vec{k},\omega) = \frac{\gamma^2_{\vec{k}}\bar{n}^2V_d^2(\vec{k})}{\Omega^2(\omega)+\gamma^2_{\vec{k}}E^2(\vec{k})} \quad (7)$$

where $\Omega(\omega) = \omega^2 - E^2(\vec{k}) + \gamma^2_{\vec{k}}/4$. which is shown in Fig.2a with different $E(\vec{k})$ and $\gamma_{\vec{k}}$.

In the strong coupling case $k < k^*, E(\vec{k}) < \gamma_{\vec{k}}/2$, $S_1(\vec{k},\omega)$ reaches the maximum $\gamma^2_{\vec{k}}\bar{n}^2V_d^2(\vec{k})/[\gamma^2_{\vec{k}}/4+E^2(\vec{k})]^2$ at $\omega_k = \mu$. As $\vec{k}\to 0$, $E(\vec{k}) = u|\vec{k}| \to 0$, then $S_1(\vec{k},\omega) \to \frac{\gamma^2_{\vec{k}}\bar{n}^2V_d^2(\vec{k})}{(\omega^2+\gamma^2_{\vec{k}}/4)^2}$, so the curve has a half width $\sim \hbar\gamma_0 \sim 10^{-4}meV$. This is expected, because the quasiparticles are not well defined with the decay rate γ_0 much larger than its energy $E(\vec{k})$. In the weak coupling case $E(\vec{k}) > \gamma_{\vec{k}}/2$, at the two resonance frequencies $\omega_k = \mu \pm [E^2(\vec{k}) - \gamma^2_{\vec{k}}/4]^{1/2}$, $S_1(\vec{k},\omega)$ reaches the maximum $\bar{n}^2V_d^2(\vec{k})/E^2(\vec{k})$. It can be shown that when $E(\vec{k}) \gg \gamma_{\vec{k}}/2$, the width of the two peaks at the two resonance frequencies is $\sim \gamma_{\vec{k}}$, this is expected, because the quasi-particle is well defined with energy $\mu \pm [E^2(\vec{k}) - \gamma^2_{\vec{k}}/4]^{1/2}$ and the half-width $\gamma_{\vec{k}}$.

The Momentum Distribution Curve (MDC) $S_1(\vec{k}) = \sum_{k_z} S_1(\vec{k},\omega) = \int d\omega_k D_{\vec{k}}(\omega_k)S_1(\vec{k},\omega)$ is:

$$S_1(\vec{k}) = \frac{D_{\vec{k}}(\mu)\bar{n}^2V_d^2(\vec{k})\gamma_{\vec{k}}}{2[E^2(\vec{k})+(\frac{\gamma_{\vec{k}}}{2})^2]} \quad (8)$$

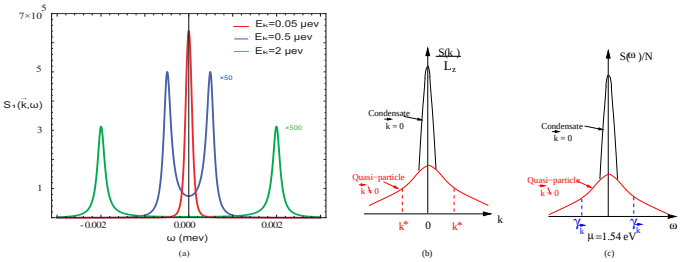

FIG. 2: (a) The angle resolved power spectrum (ARPS) of the emitted photon with in-plane momentum $\vec{k}$. When $E(\vec{k}) \le \hbar\gamma_{\vec{k}}/2$, there is only one peak with the width $\gamma_{\vec{k}}/2$. When $E(\vec{k}) > \hbar\gamma_{\vec{k}}/2$, there are two peaks at the two resonance photon frequencies $\omega_k = \mu \pm [E^2(\vec{k}) - \gamma^2_{\vec{k}}/4]^{1/2}$ also with width $\gamma_{\vec{k}}/2$. The $S_1(\vec{k},\omega)$ at $E(\vec{k}) = 0.5\mu eV$ and $E(\vec{k}) = 2\mu eV$ are multiplied by 50 and 500 in order to be seen in the figure. (b) The zero temperature MDC has a bi-model structure consisting of a sharp peak $S(\vec{k}=0)/L_z = N\gamma_0/v_g$ due to the condensate at $\vec{k}=0$ superposing on a Lorentzian peak with a half width $k^* \sim 10^2 cm^{-1}$ due to quasi-particle excitations at $\vec{k}\neq 0$. (c) The zero temperature EDC has a bi-model structure consisting of a sharp δ function peak $S(\omega)/N = \gamma_0\delta(\omega-\mu)$ due to the condensate at $\vec{k}=0$ superposing on a Lorentzian peak with the half envelop width $\gamma_{\vec{k}}/2 \sim 0.1\mu eV$ due to quasi-particle excitations at $\vec{k}\neq 0$.

which is a Lorentian with the half width at $k^* \sim 10^{-2}cm^{-1}$ shown in Fig.2b. From Eqn.4, one can see the condensate contribution at $\vec{k}=0$ is $N_{ph}/L_z = N\gamma_0/v_g \propto N$, while the contribution from the quasi-particle is $S_1(\vec{k}\to 0)/L_z = \frac{2n^2V_d^2(0)}{v_g\gamma_0} \propto n^2/\gamma_0$. We can also calculate the the one photon spacial correlation function:

$$G_1(r) \sim \int \frac{d^2\vec{k}}{(2\pi)^2}\frac{e^{i\vec{k}\cdot\vec{r}}}{k^2+k^{*2}} \sim e^{-k^*r} \quad (9)$$

where we can identify the coherence length $\xi \sim 1/k^* \sim 40\mu m$. This coherence length has been measured in [9] and will be discussed in section 7.

The Energy Distribution Curve (EDC) $S_1(\omega) = \sum_{\vec{k}} S_1(\vec{k},\omega)$ is:

$$S_1(\omega) = N\bar{n}\times\int\frac{d^2\vec{k}}{(2\pi)^2}\frac{\gamma^2_{\vec{k}}V_d^2(\vec{k})}{\Omega^2(\omega)+\gamma^2_{\vec{k}}E^2(\vec{k})} = \frac{N\bar{n}V_d^2(\vec{k}=0)}{4\pi u^2}f(\frac{|\omega|}{\gamma_{\vec{k}=0}}) \quad (10)$$

where $f(x) = \frac{1}{x}[\frac{\pi}{2} - arctg\frac{1/4-x^2}{x}]$ where $-\pi/2 < arctgy < \pi/2$. From Eqn.4, one can see the condensate contribution at $\vec{k}=0$ is $n_{\omega_{k_z}}/N = \gamma_0\delta(\omega_{k_z}-\mu)$, while the contribution from the quasi-particle $S_1(\omega=0)/N = \frac{\bar{n}V_d^2(\vec{k}=0)}{\pi u^2}$. Both are shown in the Fig.2c.

6. Quasi-particle spectrum of a non-equilibrium stationary exciton superfluid and its experimental

observation. It is important to compare the excitation spectra in Fig.1. Fig.1a is the well know quasi-particle excitations in an equilibrium superfluid. They are well defined quasi-particles with infinite lifetime. However, the quasi-particles in Fig.1c are not well defined in any length scales, because the decay rate is always much larger than the energy. Fig.1b is between the two extreme cases. When $k < k^*$, the quasi-particle is not well defined, the ARPS is centered around $\omega_k = \mu$ with the width γ_k. The MDC has large values at $k < k^*$. The EDC has large values at $\omega < \gamma_k$. When $k > k^*$, the quasi-particles is well defined, the ARPS has two well defined quasi-particles peaks at $\omega_k = \mu \pm [E^2(\vec{k}) - \gamma_{\vec{k}}^2/4]^{1/2}$ with the width γ_k. The MDC has very small values at $k > k^*$. The EDC has very small values at $\omega > \gamma_k$. So in the long wavelength $r > \xi \sim 1/k^*$ (or small momentum $k < k^*$) limit and long time $\tau > \tau_{ex} \sim 1/\gamma_k$ (or low energy limit $\omega < \gamma_k$) limit, there is not a well defined superfluid which is consistent with the results achived in [18]. However, in the distance $r < \xi \sim 1/k^*$ (or momentum $k > k^*$) limit and the time $\tau < \tau_{ex} \sim 1/\gamma_k$ (or energy scale $\omega > \gamma_k$), there is still well defined superfluid and associated quasi-particle excitations. This is the main difference and analogy between the excitation spectrum in the equilibrium superfluid in Fig.1a and that in the non-equilibrium steady state superfluid in Fig.1b. Although we derived the Fig.1b from the specific Hamiltonian Eqn.1, we expect it is universal for any stationary pumping-decay system such as exciton-polariton systems. Very recently, the elementary excitation spectrum of exciton-polariton inside a micro-cavity was measured [10] and was found to be very similar to that in a helium 4 superfluid shown in Fig.1a except in a small regime near $k = 0$. We believe this observation is precisely due to the excitation spectrum in a non-equilibrium stationary superfluid shown in Fig.1b.

7. Comments on current experiment data and possible future experiments. In [4, 5], the spatially and spectrally resolved photoluminescence intensity has a sharp peak at the emitted photon energy $E = 1.545eV$ with a width $\sim 1meV$ at the lowest temperature $\sim 1K \sim 0.1meV$. The energy conservation at $k_z = 0$ gives the maximum in-plane momentum $\vec{k}_{max} \sim 1.545eV/v_g \sim 4.3 \times 10^4 cm^{-1}$ where we used the speed of the light $v_g \simeq 8.7 \times 10^9 cm/s$ in $GaAs$ [4]. Then the maximum exciton energy $E_{max} = uk_{max} \sim 0.15meV$ where we used the spin wave velocity [4, 5] $u \sim 5 \times 10^5 cm/s$. The average lifetime of the indirect excitons in the EHBL [4, 5] is $\tau_{ex} \sim 40ns$, then we can estimate the exciton decay rate $\gamma_k \sim \hbar/40ns \sim 10^{-4}meV = 0.1\mu eV$. At the boundary of the two regimes in the Fig.1b where $E(k^*) = uk^* = \gamma_{k^*}/2 = 0.1\mu eV$, we can extract $k^* = 2.4 \times 10^2 cm^{-1} \ll k_{max}$. The typical exciton cloud size $L \sim 30\mu m$ [4]. The number of excitons is $N = nL^2 \sim 10^5$ which is comparable to the number of cold atoms inside a trap in most cold atom experiments. The central peak due to the condensate in the MDC Fig.2b is broadened to $k_0 \sim 1/L \sim 10^3 cm^{-1}$ which is already larger than the half width due to the quasi-particle $k^* \sim 10^2 cm^{-1}$. So it is impossible to distinguish the bi-model structure in the MDC in Fig.2b at such a small exciton size. The coherence length was measured in [9]. From Eqn.9, we find the coherence $\xi \sim 1/k^* \sim 40\mu m$ which is slightly larger than the exciton cloud size $L \sim 30\mu m$. It is easy to see that the central peak due to the condensate in the EDC in the Fig.2a is broadened simply due to the change of the local chemical potential from the center to the edge of the trap $\Delta\omega = \frac{1}{2}u_0 L^2 \sim 0.1meV$ where $u_0 \sim 10^{-12} eV nm^{-2}$ [4, 5]. This value is much larger than the half width due to the quasi-particle $\gamma_{\vec{k}} \sim 0.1\mu eV$, so it is impossible to distinguish the bi-model structure in the EDC in Fig.2c either. In order to understand if the observed peak is indeed due to the exciton condensate, one has to study how the bi-model structures shown in Fig.2 will change inside a harmonic trap at a finite temperature $\sim 1K$ and the effects of both dark and bright excitons. This will be discussed in a separate publication. The fine structures in the ARPS in the Fig.2a and phase sensitive homodyne measurement [11] are also needed to test any existence of the exciton condensate.

8. Conclusions We study the power spectrum of photons emitted from the exciton superfluid phase in semiconductor electron-hole bilayer systems. We find that the photons emitted along the direction perpendicular to the layer are in a coherent state which possesses several remarkable properties, while those along all tilted directions due to the quasi-particles above the condensate show very interesting structures. We determined the angle resolved power spectrum (ARPS), the line shapes of both the MDC and the EDC. We also pointed out the analogy and difference between the quasi-particles in an equilibrium superfluid and those in a non-equilibrium stationary superfluid. This difference precisely explained the recent experimental observation of excitation spectrum of exciton polariton in a planar microcavity. We commented on available experimental data both MDC and EDC and also suggested possible future ARPS experiment to test our theoretical predictions

We are very grateful for C.P. Sun for many helpful suggestions and encouragements. We also thank Peng Zhang for helpful discussions. J.Ye is indebted to B. Halperin for critical reading of the manuscript and many helpful suggestions. J. Ye is grateful for A. V. Balatsky, L. Butov, Jason Ho, Guoxinag Huang, Xuedong Hu, Allan Macdonald, G. Murthy, Zhibing Li, Qian Niu, Zhe-Yu Oh, Lu Sham, D. Snoke, Hailing Wang, Congjun Wu, C. L Yang, Wang Yao, Fuchun Zhang, Weiping Zhang for helpful discussions. J. Ye's research at KITP-C was supported by the Project of Knowledge Innovation Program (PKIP) of Chinese Academy of Sciences; at KITP was supported in part by the NSF under grant No. PHY-0551164.

[1] John M. Blatt, K. W. Böer and Werner Brandt, Phys. Rev. 126, 1691 (1962).

[2] L. V. Keldysh and A. N. Kozlov. *Sov, Phys. JETP* 27, 521-528 (1968).

[3] Yu. E. Lozovik and V. I. Yudson, Pis'ma Zh. Eksp. Teor. Fiz. 22, 556 (1975) [JETP Lett. 22, 274 (1975)]

[4] L. V. Butov, *et al*, Nature 417, 47 - 52 (02 May 2002); Nature 418, 751 - 754 (15 Aug 2002); C. W. Lai, *et al* Science 23 January 2004 303: 503-506.

[5] D. Snoke, *et al* Nature 418, 754 - 757 (15 Aug 2002); David Snoke, Nature 443, 403 - 404 (28 Sep 2006);

[6] U. Sivan, P. M. Solomon, and H. Shtrikman, Phys. Rev. Lett. 68, 1196 - 1199 (1992)

[7] J. A. Seamons, D. R. Tibbetts, J. L. Reno, M. P. Lilly, arXiv:cond-mat/0611220.

[8] R. Rapaport, *et al*, Phys. Rev. Lett. 92, 117405 (2004); Phys. Rev. B 72, 075428 (2005).

[9] Sen Yang, A. T. Hammack, M. M. Fogler, and L. V. Butov, Phys. Rev. Lett 97, 187402 (2006).

[10] S. Utsunomiya, *et al* , Nature Physics 4, 700 - 705 (01 Sep 2008).

[11] Tao Shi, Jinwu Ye, Longhua Jiang and C.P. Sun, unpublished.

[12] Jinwu Ye, arXiv:cond-mat/0712.0437.

[13] Jinwu Ye and Longhua Jiang, Phys. Rev. Lett. 98, 236802 (2007), Jinwu Ye, Phys. Rev. Lett. 97, 236803 (2006), Jinwu Ye, Annals of Physics, 323 (2008), 580-630.

[14] P. Mehta and N. Andrei, Phys. Rev. Lett. 100, 086804 (2008); *ibid*, 96, 216802 (2006).

[15] In order to keep the relative energy difference between the exciton and the photon intact, we made a rotation $a = \tilde{a}e^{-i\mu t}$ and neglected the ˜ in the following.

[16] This straightforward conclusion was reached in Y. Yamamoto and A. Imamoglu, Mesoscopic quantum optics, John Wiley & Sons, Inc. 1999. P213. A. Castro *et.al*, PRL 87, 246403. But the results achieved at $\vec{k} = 0$ in the rest of the following section are highly non-trvial and completely new. The results on $\vec{k} \neq 0$ achieved in the other sections are also completely new.

[17] D. F. Walls and G. J. Milburn, Quantum Optics, Springer-Verlag, 1994. Chap.7.

[18] W. Kohn and D. Shrrington, Rev. Mod. Phys. 42, 1-11 (1970).